Translation Initiation Factor (eIF) 4B Affects the Rates of Binding of the mRNA m^{7}G Cap Analogue to Wheat Germ eIFiso4F and eIFiso4F·PABP†

Mateen A. Khan and Dixie J. Goss*

Department of Chemistry, Hunter College and Graduate Center of the City University of New York, New York, New York 10021

Received December 23, 2004; Revised Manuscript Received January 20, 2005

ABSTRACT: Previous kinetic binding studies of wheat germ protein synthesis eukaryotic translational initiation factor eIFiso4F and its subunit, eIFiso4E, with m^{7}GTP and mRNA analogues indicated that binding occurred by a two-step process with the first step occurring at a rate close to the diffusion-controlled rate [Sha, M., Wang, Y., Xiang, T., van Heerden, A., Browning, K. S., and Goss, D. J. (1995) *J. Biol. Chem*. *270*, 29904−29909]. The kinetic effects of eIF4B, PABP, and wheat germ eIFiso4F with two mRNA cap analogues and the temperature dependence of this reaction were measured and compared. The Arrhenius activation energies for binding of the two mRNA cap analogues, Ant-m^{7}GTP and m^{7}GpppG, were significantly different. Fluorescence stopped-flow studies of the eIFiso4F·eIF4B protein complex with two m^{7}G cap analogues show a concentration-independent conformational change. The rate of this conformational change was approximately 2.4-fold faster for the eIFiso4F·eIF4B complex compared with our previous studies of eIFiso4F [Sha, M., Wang, Y., Xiang, T., van Heerden, A., Browning, K. S., and Goss, D. J. (1995) *J. Biol. Chem*. *270*, 29904−29909]. The dissociation rates were 3.7- and 5.4-fold slower for eIFiso4F·Ant-m^{7}GTP and eIFiso4F·m^{7}GpppG, respectively, in the presence of eIF4B and PABP. These studies show that eIF4B and PABP enhance the interaction with the cap and probably are involved in protein−protein interactions as well. The temperature dependence of the cap binding reaction was markedly reduced in the presence of either eIF4B or PABP. However, when both eIF4B and PABP were present, not only was the energy barrier reduced but the binding rate was faster. Since cap binding is thought to be the rate-limiting step in protein synthesis, these two proteins may perform a critical function in regulation of the overall protein synthesis efficiency. This suggests that the presence of both proteins leads to a rapid, stable complex, which serves as a scaffold for further initiation complex formation.

Initiation of protein synthesis requires assembly of a large protein−nucleic complex. Eukaryotic translation initiation factor (eIF)[1] 4F is a protein complex that mediates recruitment of the ribosome to mRNA. This event is the rate-limiting step for translation under most circumstances, yet little is known about the kinetics of this process (*2*−*6*). In most eukaryotes, mRNA is required to have both a 5′ cap (m^{7}GpppX) and a poly(A) tail for efficient translation and message stability (*7*−*12*). These two elements act synergistically to increase translational efficiency, and evidence suggests that they communicate during translation (*13*−*15*). The cap serves as the binding site for initiation factors eIF4F and eIFiso4F, an isozyme form of eIF4F present in higher plants. The small subunit of eIF4F (eIF4E) recognizes the cap structure. eIF4F interacts with the poly(A) binding protein (PABP) through the eIF4G subunit, the larger subunit of eIF4F or eIFiso4F. eIF4G in turn recruits other initiation factors, such as eIF3, eIF4A, and PABP, to the 5′ end of the mRNA, to generate the cap-binding complex. The cap-associated proteins have a very high affinity for PABP in the absence of poly(A) in the wheat germ system (*15*) but require poly(A) in yeast (*14*). Binding of eIF4F, eIFiso4F, eIF4B, and eIF4A is believed to catalyze the efficient unwinding of secondary structure in the 5′-untranslated region (*16*). In combination with PABPs, these factors promote the functional circularization of mRNA believed to be necessary for efficient translation (*17*−*21*).

In wheat germ and other plants, an isozyme form of eIF4F called eIFiso4F has been found (*22*). The function of eIFiso4F is indistinguishable from that of eIF4F in supporting cap-dependent in vitro translation (*23*). eIFiso4F contains two subunits, a 28 kDa eIFiso4E subunit and an 86 kDa eIFiso4G subunit. eIFiso4E acts as the binding site of the m^{7}GpppN cap. eIFiso4G binds to mRNA in an ATP-dependent manner, may interact with eIF4A and eIF4B (*24*), and, more interestingly, may interact with PABP (*15*, *25*).

† This work was supported in part by National Science Foundation Grant MCB 0413982 (to D.J.G.) and a Professional Staff Congress City University of New York faculty award (to D.J.G.). Research Center in Minority Institution Award RR-03037 from the National Center for Research Resources of the National Institutes of Health supports infrastructure at Hunter College.

* To whom correspondence should be addressed: Department of Chemistry, Hunter College of the City University of New York, New York, NY 10021. Telephone: (212) 772-5383. Fax: (212) 772-5332. E-mail: dgoss@hunter.cuny.edu.

[1] Abbreviations: eIF, eukaryotic initiation factor; PABP, poly(A) binding protein; Ant-m^{7}GTP, anthraniloyl-7-methylguanosine triphosphate; HEPES, 4-(2-hydroxyethyl)-1-piperazineethanesulfonic acid; EDTA, ethylenediaminetetraacetic acid; DTT, dithiothreitol; PMSF, phenylmethanesulfonyl fluoride; SDS, sodium dodecyl sulfate; Tris, tris(hydroxymethyl)aminomethane.

10.1021/bi047298g CCC: $30.25
Published on Web 02/25/2005

Wheat germ eIF4F consists of only two subunits, a 26 kDa eIF4E subunit and a 220 kDa eIF4G subunit in a 1:1 molar ratio. Some structural and functional similarity exists between eIF4F and eIFiso4F. Both wheat germ eIF4F and eIFiso4F have RNA-dependent ATPase activity. Only one wheat germ factor is required for ATP hydrolysis and stimulation of protein synthesis in an eIF4F or eIFiso4F deficient translation system (*26*, *27*). eIF4F was also found to be functionally and physically similar to mammalian eIF4F except that it lacks an eIF4A-like subunit (*26*, *28*). Functionally, eIFiso4F is very similar to eIF4F even though these two proteins are antigenically distinct (*26*). Wheat germ eIFiso4F can substitute for mammalian eIF4F in an RNA-dependent ATPase activity and in cross-linking of mammalian eIF4A to the cap of oxidized mRNA (*29*).

PABP has been shown to be necessary for 40S ribosomal subunits binding to an mRNA and for formation of the 48S initiation complex (*14*, *30*). PABP·eIFiso4F interaction has been shown to enhance the binding affinity of both cap analogues and poly(A) by ~40-fold (*25*). Further studies have shown that the cap and poly(A) tail can be bound by the protein complex simultaneously (*25*). It was concluded that the increased binding affinity for the 5′ cap by the protein complex could account for at least part of the enhancement of translation. We have previously investigated the mechanism of eIFiso4F and eIFiso4E interacting with the cap (*1*). Kinetic studies indicated that the binding involved a two-step process with the first reaction being too fast to assess via stopped-flow techniques. The second reaction, a conformational change, was ~10-fold faster for eIFiso4E than for eIFiso4F. To understand the assembly of the initiation complex, we have begun to investigate the effects of other proteins on cap binding kinetics. The aim of this study is to investigate the effects of eIF4B on the binding activity of eIFiso4F in the presence and absence of the poly(A) binding protein (PABP) and to determine the activation energy of these reactions.

EXPERIMENTAL PROCEDURES

Materials. m^7GTP and m^7GpppG were purchased from Sigma (St. Louis, MO). Ant-m^7GTP was synthesized and purified as described previously (*31*). The concentration of Ant-m^7GTP was determined spectrophotometrically using an absorption coefficient ϵ_{332} of 4600 M^{-1} cm^{-1}.

Expression and Purification of Recombinant Proteins. eIFiso4E, eIFiso4G, and eIF4B were expressed in *Escherichia coli* containing the constructed pET3d vector in BL21-(DE3) pLys as described elsewhere (*32*). HiTrap Mono-Q ion exchange and m^7GTP−Sepharose columns (Pharmacia Biotech, Inc.) were used for the purification of eIFiso4E. *E. coli* cells were disrupted by sonication and suspended in buffer B-600 [20 mM Hepes/KOH (pH 7.6), 1 mM DTT, 0.1 mM EDTA, 10% glycerol, and 600 mM KCl] containing 0.5 mM phenylmethanesulfonyl fluoride (PMSF), 0.5 mL of aprotinin, and 100 μg/mL soybean trypsin inhibitor. The lysed cells were centrifuged at 15 000 rpm in a Sorvall SS-34 rotor for 30 min (S11 supernatant) to separate soluble eIFiso4E from inclusion bodies. The S11 supernatant was centrifuged at 45 000 rpm in a Sorvall TV-850 rotor for 3 h (S175 supernatant) to remove ribosomes and additional aggregates. The S175 supernatant was dialyzed against buffer B-50 [50 mM Hepes/KOH (pH 7.0), 10% glycerol, 1 mM DTT, 0.1 mM EDTA, and 50 mM KCl]. The dialyzed sample was applied to a 5 mL HiTrap Mono-Q column equilibrated with 10 bed volumes of buffer B-50 with a flow rate of 2 mL/min. The column was washed at the same flow rate with buffer B-50 until the optical density returned to baseline. The expressed eIFiso4E was eluted with a 50 to 400 mM KCl linear gradient at a flow rate of 2 mL/min. The peak was collected in 1.0 mL fractions. To maximize purity, the sample was subsequently applied to a 4 mL m^7GTP−Sepharose column (Pharmacia Biotech) equilibrated in buffer B-50. The column was washed with buffer B-50, followed by 25 mL of buffer B-50 containing 0.1 mM GTP to remove GTP-binding proteins. The expressed eIFiso4E was eluted from the column with 15 mL of buffer B-50 containing 100 mM GTP. After 2 mL of the elution buffer had entered the column, the column was turned off for 30 min. Elution was resumed, and column fractions (0.5 mL) were collected. The fractions were analyzed by 10% SDS−polyacrylamide gel electrophoresis. A HiTrap SP column (Amersham Pharmacia Biotech) was used to purify eIFiso4G and eIF4B by the following procedure. *E. coli* cells were disrupted by alumina, suspended in buffer B-600, and centrifuged at 45 000 rpm for 2 h. The supernatant was dialyzed against buffer B-50 and loaded onto a 5 mL HiTrap SP column and washed with B-50 buffer until the optical density returned to the baseline. A 50 to 400 mM KCl linear gradient (total volume of 100 mL) was used to elute the proteins, and 1.0 mL fractions were collected. The proteins appeared in the 200−300 mM KCl fractions. After purification, the purity was confirmed by 10% SDS−polyacrylamide gel electrophoresis. All steps were carried out in a cold box at approximately 5 °C. The pH of buffer B-50 used for eIF4B purification was 7.5.

PABP was expressed in *E. coli* containing the constructed pET19b vector in BL21(DE3) pLys as described elsewhere (*32*), and the tagged protein was purified in 20 mM Tris-HCl (pH 7.9), 500 mM NaCl, and 100 mM imidazole by the His-bind kit protocol (Novagen). The protein was >95% pure as determined by 10% SDS−polyacrylamide gel electrophoresis with Coomassie Brilliant Blue staining.

All samples were dialyzed against buffer B [20 mM HEPES/KOH, 100 mM KCl, 1.0 mM $MgCl_2$, 1.0 mM dithiothreitol, and 1.0 mM EDTA (pH 7.6)] and passed through a 0.22 μm filter (Millipore) before the spectroscopy measurements were performed. The fractions were concentrated with a Centriplus YM-10 filter (Amicon Co.) as necessary. The protein concentrations were determined by a Bradford assay with bovine serum albumin as the standard (*33*) using a Bio-Rad protein assay reagent (Bio-Rad Laboratories, Hercules, CA).

Spectroscopy Measurements. Absorbance measurements were obtained using a Cary-3 double-beam UV−visible spectrophotometer. Fluorescence spectra were recorded on a Spex Fluorog τ2 spectrofluorometer equipped with excitation and emission polarizers. All measurements were performed at 22 °C except as noted.

Stopped-Flow Fluorescence Kinetics. Stopped-flow fluorescence experiments were performed on an OLIS RSM 1000 stopped-flow system with a dead time of 1 ms. The excitation wavelength was 332 nm, and the emission was monitored after the light passed through a 400 nm cut-on filter (provided by OLIS Inc.) for eIF·Ant-m^7GTP. The excitation wave-

length was 280 nm, and the cut-on filter was 324 nm for eIF·m^{7}GpppG interactions. A reference photomultiplier was used to monitor fluctuations in the lamp intensity. The temperature of the flow cell and solution reservoirs was maintained using a temperature-controlled circulating water bath. As described elsewhere (*31*, *34*, *35*), eIFiso4F binding induced an increase in Ant-m^{7}GTP fluorescence. After 2 μM (each) eIFiso4F, eIFiso4F·eIF4B, eIFiso4F·PABP, or eIFiso4F·eIF4B·PABP had been rapidly mixed with 10 μM Ant-m^7-GTP or m^{7}GpppG cap, the time course of the fluorescence intensity change was recorded by computer data acquisition. In each experiment, 1000 pairs of data were recorded, and sets of data from three experiments were averaged. Each averaged set of stopped-flow data was then fitted to nonlinear analytical equations using Global analysis software provided by OLIS. Fitted curves correspond to the following single-exponential equation (*36*)

$$\Delta F_t = \Delta F_\infty[1 - \exp(-k_{obs}t)] \quad (1)$$

where ΔF_t is that fluorescence observed at any time t and the final fluorescence when the reaction achieves equilibrium, ΔF_∞ is the difference between m^{7}G cap fluorescence at time zero and equilibrium, and k_{obs} is the observed first-order rate constant. The reaction was consistent with a single-exponential process. The derived rate constants were used to construct an Arrhenius plot according to the equation

$$\ln k = -\frac{E_a}{RT} + \ln A \quad (2)$$

where k is the rate constant, E_a is the activation energy, and A is the Arrhenius pre-exponential term. The activation energy was calculated from the slope of the fitted linear plot of ln k versus $1/T$ (kelvin).

Dissociation Rate Constants. To measure the dissociation rate constants, a complex of the mRNA cap analogue, Ant-m^{7}GTP or m^{7}GpppG, with either eIFiso4F, eIFiso4F·eIF4B, eIFiso4F·PABP, or eIFiso4F·eIF4B·PABP was rapidly diluted 15-fold in a spectrofluorimeter cuvette, and the resulting decrease in fluorescence was measured. Because of the high binding affinity of the mRNA cap analogue for the complex, a large dilution, which could not be accomplished by stopped-flow methods, was necessary. The concentrations of the reactants before mixing were 25 μM for the mRNA cap analogue and 5 μM (each) for eIFiso4F, eIF4B, and PABP. The diluting buffer contained the same concentration of eIF4B or PABP (as in reaction mixture) to prevent protein complex dissociation. The dissociation rates were determined from fits of the appropriate equations to the data using nonlinear least-squares fitting program KaleidaGraph (version 2.1.3, Abelbeck Software).

RESULTS

The stopped-flow data for the binding of the two mRNA cap analogues, a mononucleotide cap Ant-m^{7}GTP and dinucleotide cap m^{7}GpppG, to the eIFs complex were plotted as the relative voltage, which is proportional to fluorescence intensity versus time as shown in Figures 1 and 2. Time course data were fitted by nonlinear regression analysis (*36*) assuming a single-exponential change. Addition of eIF4B to the eIFiso4F·PABP complex increased the rate constant

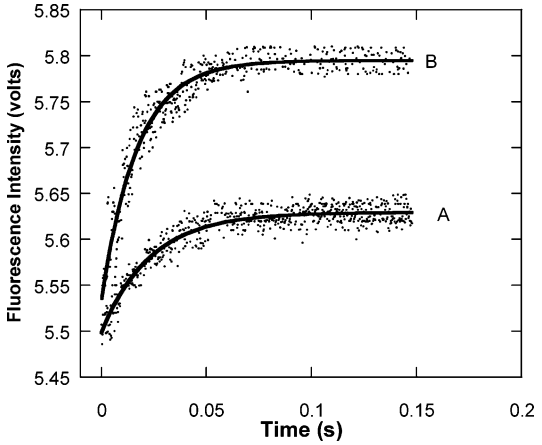

FIGURE 1: Typical time courses of eIFiso4F·PABP, eIFiso4F·4B·PABP, and Ant-m^{7}GTP interactions. The excitation wavelength was 332 nm. The signal represents the total fluorescence emission above 400 nm. Solutions of (A) 2 μM eIFiso4F·PABP (1 μM after mixing) and (B) 2 μM eIFiso4F·4B·PABP (1 μM after mixing) were mixed with a solution of 10 μM Ant-m^{7}GTP (5 μM after mixing) in a stopped-flow apparatus at 22 °C. The fitted curve corresponds to an overall first-order process (eq 1).

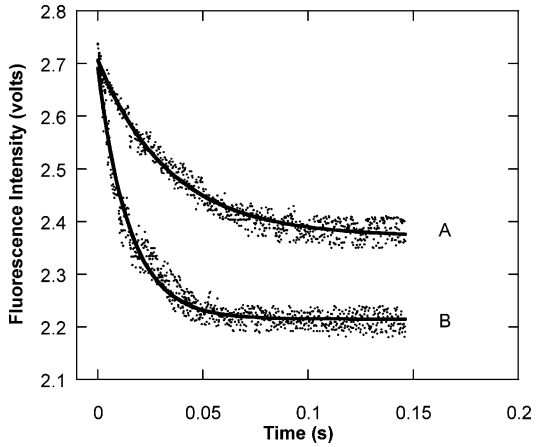

FIGURE 2: Typical time course of the intrinsic protein fluorescence intensity decrease caused by binding of (A) eIFiso4F·PABP and (B) eIFiso4F·4B·PABP to m^{7}GpppG. The excitation wavelength was 280 nm. The signal represents the total fluorescence emission above 324 nm. The final concentrations were 1 μM (each) eIFiso4F, eIF4B, and PABP and 5 μM m^{7}GpppG at pH 7.6 and 22 °C. The fitted curve corresponds to an overall first-order process (eq 1).

(k_2) for Ant-m^{7}GTP binding ~1.5-fold (k_2 = 39.0 s^{-1} for eIFiso4F·PABP; k_2 = 60.5 ± 1.5 for eIFiso4F·eIF4B·PABP) (Figure 1). However, the effect of eIF4B on the eIFiso4F·PABP complex binding with m^{7}GpppG cap increased k_2 more than 2-fold (k_2 = 29.2 ± 0.55 s^{-1} for eIFiso4F·PABP; k_2 = 66.58 ± 0.99 s^{-1} for eIFiso4F·eIF4B·PABP) (Figure 2). These data show that eIF4B has a greater effect on eIFiso4F·PABP binding to the dinucleotide cap than to the mononucleotide cap. Our previous studies have shown that eIF4B had an effect on cap binding; however, PABP had a much larger effect on the equilibrium for the cap binding with eIFiso4F. The K_{eq} values were (27.10 ± 0.49) × 10^6, (34.48 ± 0.55) × 10^6, and (232.55 ± 1.9) × 10^6 M^{-1} for eIFiso4F, eIFiso4F·eIF4B, and eIFiso4F·PABP, respectively (*25*, *37*).

Under the pseudo-first-order conditions, where mRNA cap was in excess, the observed pseudo-first-order rate constant is predicted to be a linear function of the concentration of

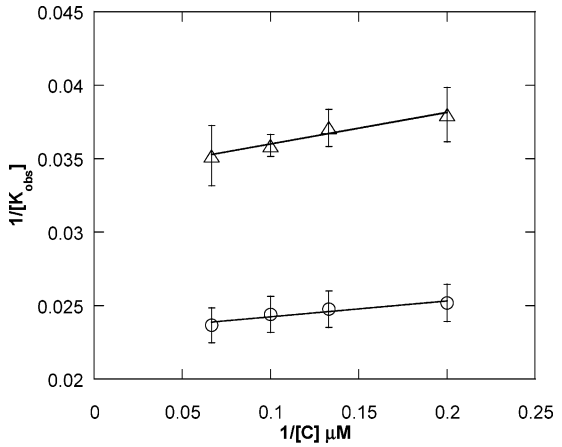

FIGURE 3: Kinetic plots of $1/k_{obs}$ vs 1/[C] of 1 μM eIFiso4F·4B at different Ant-m^{7}GTP (○) and m^{7}GpppG (△) concentrations (5.0, 7.5, 10.0, and 15.0 μM) at 22 °C. k_2 was obtained as the reciprocal of the *Y*-intercept (43.19 ± 2.57 s^{-1} for eIFiso4F·4B·Ant-m^{7}GTP and 29.52 ± 1.65 s^{-1} for eIFiso4F·4B·m^{7}GpppG).

Table 1: Kinetic Binding Constants for the Interaction of eIFiso4F·eIF4B and eIFiso4F·eIF4B·PABP with the Ant-m^{7}GTP Cap

	rate constant k_2 (s^{-1})			
temp (°C)	eIFiso4F[a]	eIFiso4F·4B	eIFiso4F·PABP[a]	eIFiso4F·4B·PABP
4	4.42	9.08 ± 0.5	14.0	23.5 ± 1.1
10	9.36	15.0 ± 0.8	20.0	35.0 ± 1.7
15	17.1	20.9 ± 0.7	28.5	40.8 ± 2.3
22	37.9	39.6 ± 1.1	39.0	60.5 ± 1.5
31	102	69.0 ± 2.6	62.2	81.1 ± 6.2
E_a (kJ/mol)	81.5 ± 2.5	53.27 ± 2.7	39.8 ± 1.6	29.22 ± 1.32
dissociation rate k_{-2} ($\times 10^3$ s^{-1})	37.21 ± 1.3	24.16 ± 1.2	13.74 ± 0.5	10.03 ± 0.31

[a] Values obtained from ref *38*.

Ant-m^{7}GTP or m^{7}GpppG. However, as observed previously (*1*, *38*), the binding rates depended little on mRNA cap concentration over a concentration range of 5−15 μM, a 4−14-fold excess. The observed rate varied from 39.6 to 42.25 s^{-1} for Ant-m^{7}GTP and from 26.31 to 28.40 s^{-1} for m^{7}GpppG with eIFiso4F·4B. As proposed previously (*1*, *39*), the binding mechanisms can be explained by a two-step process involving a fast association of eIFiso4F·4B and the mRNA cap followed by a slow change in conformation from the first association complex to the stable complex.

The binding rates have a relationship with the concentration of substrate as described previously (*36*), $1/k_{obs} = 1/k_2 + K_1/k_2[C]$, where k_{obs} is the observed first-order rate constant, k_2 is the forward rate constant for the second step, and [C] is the concentration of Ant-m^{7}GTP or m^{7}GpppG. Figure 3 is a plot of $1/k_{obs}$ versus 1/[C] for eIFiso4F·4B, which shows the predicted linear relationship. From the intercept of $1/k_2$, k_2 was found to 43.19 ± 2.6 and 29.52 ± 1.65 s^{-1} for Ant-m^{7}GTP and m^{7}GpppG with eIFiso4F·4B, respectively.

The effects of eIF4B on the rate of binding of eIFiso4F and eIFiso4F·PABP to the two mRNA cap analogues, Ant-m^{7}GTP and m^{7}GpppG, at different temperatures are shown in Tables 1 and 2. Addition of eIF4B to the eIFiso4F and eIFiso4F·PABP complex increased k_2 values. Similarly, the k_2 values for protein complexes with the mRNA cap

Table 2: Kinetic Binding Constants for the Interaction of eIFiso4F, eIFiso4F·4B, eIFiso4F·PABP, and eIFiso4F·4B·PABP with the m^{7}GpppG Cap

	rate constant k_2 (s^{-1})			
temp (°C)	eIFiso4F	eIFiso4F·4B	eIFiso4F·PABP	eIFiso4F·4B·PABP
4	3.43 ± 0.09	8.14 ± 0.86	13.2 ± 0.76	28.67 ± 2.67
10	6.42 ± 0.32	12.63 ± 0.64	18.07 ± 0.55	35.37 ± 1.06
15	10.59 ± 0.22	17.53 ± 0.95	24.94 ± 1.74	47.28 ± 3.33
22	14.35 ± 0.63	26.31 ± 2.18	29.2 ± 0.55	66.58 ± 0.99
31	36.67 ± 0.98	48.13 ± 1.79	42.5 ± 3.73	76.80 ± 1.98
E_a (kJ/mol)	60.11 ± 2.93	45.54 ± 2.96	30.13 ± 1.56	26.04 ± 1.76
dissociation rate k_{-2} ($\times 10^3$ s^{-1})	38.8 ± 0.83	20.6 ± 0.49	14.3 ± 0.76	7.26 ± 0.44

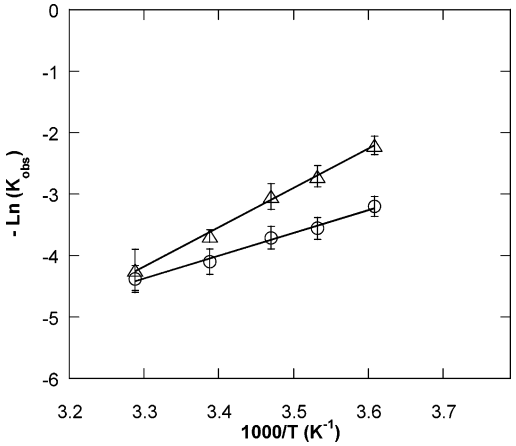

FIGURE 4: Arrhenius plots for the interaction between eIFiso4F·4B (△) and eIFiso4F·4B·PABP (○) and Ant-m^{7}GTP.

increased with an increase in temperature (Tables 1 and 2). The stopped-flow kinetic data showed that at 22 °C the binding of eIFiso4F·4B·PABP to the m^{7}GpppG cap changed the conformation approximately 4.6 times faster than the binding of eIFiso4F (k_2 = 14.35 ± 0.63 s^{-1} for eIFiso4F; k_2 = 66.58 ± 0.99 s^{-1} for eIFiso4F·4B·PABP). However, at the same temperature, the rate constant for binding of eIFiso4F·4B·PABP to Ant-m^{7}GTP, the mononucleotide cap, was only approximately 1.5 times faster than that of eIFiso4F (k_2 = 60.5 ± 1.5 s^{-1} for eIFiso4F·4B·PABP; k_2 = 37.9 s^{-1} for eIFiso4F). eIF4B has a greater effect on binding of eIFiso4F to the dinucleotide cap than to the mononucleotide cap.

The rate constant values (Tables 1 and 2) were used to construct Arrhenius plots (Figures 4 and 5) according to eq 2. The activation energies were calculated from the fitted slopes of ln *k* versus 1/*T* (kelvin). The activation energies for binding of Ant-m^{7}GTP to eIFiso4F, eIFiso4F·4B, and eIFiso4F·4B·PABP, determined from the temperature dependence of the rate constants, are shown in Table 1. After addition of eIF4B to eIFiso4F·PABP under conditions where a complex is formed, the activation energy decreased to 29.22 ± 1.32 and 26.04 ± 1.76 kJ/mol for Ant-m^{7}GTP (Figure 4) and m^{7}GpppG (Figure 5), respectively. Previous results (*38*) have shown that the activation energy for eIFiso4F (81.5 ± 2.5 kJ/mol) is ~3-fold higher than for the eIFiso4F·4B·PABP and Ant-m^{7}GTP interactions. The activation energy for binding of the dinucleotide cap m^{7}GpppG to eIFiso4F (60.11 ± 2.93 kJ/mol) is 2.3-fold higher than that of eIFiso4F·4B·PABP (26.04 ± 1.76 kJ/mol). These data show a large

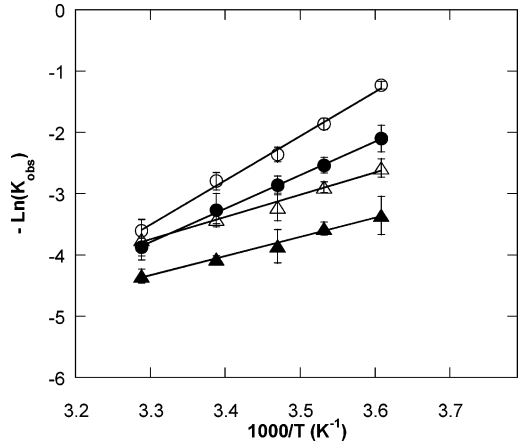

FIGURE 5: Arrhenius plots for determining the activation energy of the interaction between eIFiso4F (○), eIFiso4F·4B (●), eIFiso4F·PABP (△), and eIFiso4F·4B·PABP (▲) and m^{7}GpppG.

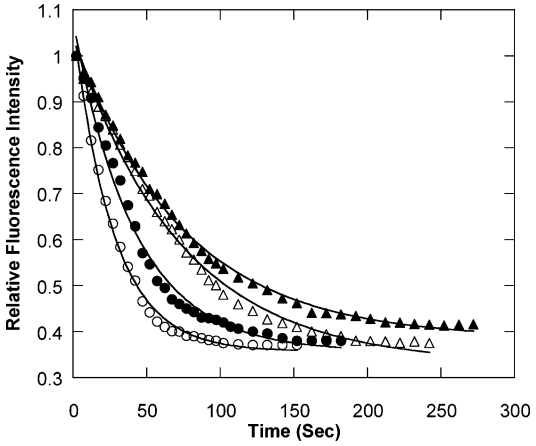

FIGURE 6: Kinetics of dissociation of Ant-m^{7}GTP from eIFiso4F·Ant-m^{7}GTP (○), eIFiso4F·4B·Ant-m^{7}GTP (●), eIFiso4F·PABP·Ant-m^{7}GTP (△), or eIFiso4F·4B·PABP·Ant-m^{7}GTP (▲) at 20 °C. Off rates were monitored by rapidly diluting 100 μL of the complex with 1500 μL of buffer. The concentrations of reactants before mixing were as follows: 25 μM Ant-m^{7}GTP, 5 μM eIFiso4F, 5 μM eIF4B, and 5 μM PABP. The diluting buffer contained the same concentration of eIF4B and/or PABP (as in the reaction mixture) to prevent protein complex dissociation. The fluorescence of Ant-m^{7}GTP was monitored.

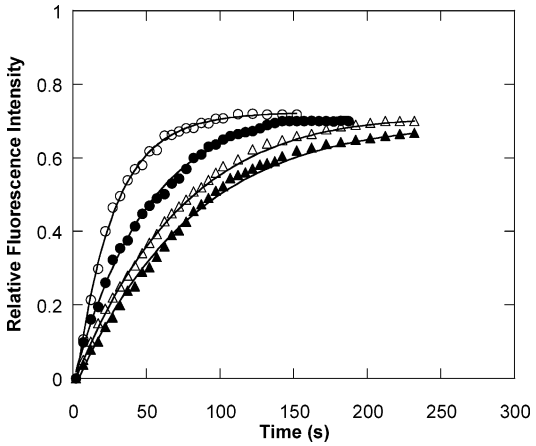

FIGURE 7: Kinetics of dissociation of m^{7}GpppG from eIFiso4F·m^{7}GpppG (○), eIFiso4F·4B·m^{7}GpppG (●), eIFiso4F·PABP·m^7-GpppG (△), or eIFiso4F·4B·PABP·m^{7}GpppG (▲) at 20 °C. Off rates were monitored by rapidly diluting 100 μL of the complex with 1500 μL of buffer. The concentrations of reactants before mixing were as follows: 25 μM m^{7}GpppG, 5 μM eIFiso4F, 5 μM eIF4B, and 5 μM PABP. The diluting buffer contained the same concentration of eIF4B and/or PABP (as in the reaction mixture) to prevent protein complex dissociation. The protein fluorescence was monitored as described in Materials and Methods.

reduction in activation energy when eIF4B alone or in combination with PABP is present. The overall reduction in activation energy for Ant-m^{7}GTP binding of 50 kJ/mol suggests a number of more favorable hydrogen bonds are formed in the transition state. The activation energy is related to the enthalpy of reaction, suggesting hydrogen bonds or ionic interactions rather than hydrophobic forces, which usually are entropically favorable, are involved. A smaller reduction in activation energy is seen for the dinucleotide cap. However, the activation energies for binding of the eIFiso4F·4B·PABP complex to the mono- or dinucleotide cap are similar. This suggests that the second base in the dinucleotide cap has a large influence on the initial binding to eIFiso4F, but is less important when the other proteins interact.

eIF4B has been shown to affect the equilibrium binding affinity of eIFiso4F·PABP for cap analogues (*15*). A substantial contribution to the equilibrium binding affinity was due to the dissociation rate. To understand further the mechanism of this reaction, the effects of eIF4B on the dissociation (k_{-2}) kinetics of the reaction were investigated. The dissociation reaction was monitored as described in Materials and Methods. Figures 6 and 7 show the results of the dilution experiment. The dissociation rate constants were obtained from the fitted curves as $(37.21 \pm 1.3) \times 10^{-3}$ and $(10.03 \pm 0.31) \times 10^{-3}$ s^{-1} for eIFiso4F and eIFiso4F·4B·PABP, respectively, with Ant-m^{7}GTP (Table 1). Similarly, the dissociation rates for eIFiso4F and eIFiso4F·4B·PABP with m^{7}GpppG were $(38.8 \pm 0.83) \times 10^{-3}$ and $(7.26 \pm 0.44) \times 10^{-3}$ s^{-1}, respectively (Table 2). Addition of eIF4B to eIFiso4F and eIFiso4F·PABP decreased the dissociation rate approximately 1.5- and 2.0-fold, respectively, for the two mRNA cap analogues.

DISCUSSION

In this study, the pre-steady-state kinetic effects of eIF4B on the binding of eIFiso4F and the eIFiso4F·PABP complex by two mRNA cap analogues, Ant-m^{7}GTP and m^{7}GpppG, were investigated using stopped-flow fluorescence. The concentration dependencies of the observed rates of this process correspond with a two-step reaction model in which initial fast association of m^{7}G cap is followed by a conformational change of the complex in a rather fast step, but with a measurable rate (k_2, Tables 1 and 2).

The mechanism of interaction of the cap with eIFiso4F·4B and eIFiso4F·4B·PABP is consistent with the previous mechanism (*38*) for interaction of the cap with eIFiso4E and eIFiso4F. The binding mechanism for cap binding to the protein complex follows a two-step process; the first step was very fast and close to the diffusion-controlled rate, and the second step was independent of concentration. In our previous studies with a dinucleotide cap analogue, we found k_2 to be almost 10-fold faster for eIFiso4E than for eIFiso4F, suggesting that the smaller protein was more able to accomplish the conformational change necessary for binding, although the equilibrium constants were similar for the two proteins.

Interestingly, eIF4B and PABP have a stronger effect on the dinucleotide cap binding than on the mononucleotide cap. Ant-m^{7}GTP binding was enhanced less than 2-fold when both proteins were present (22 °C), whereas the dinucleotide binding was enhanced almost 5-fold when both proteins were present. The fact that the rate constants, k_2, for the eIFiso4F and eIFiso4F·4B·PABP complex are less than 2-fold different for the mononucleotide analogue indicates that the second base must play a role in the binding. In the case of eIFiso4F, the second base slows the binding compared with the mononucleotide. However, the complex and also eIFiso4E bind the dinucleotide much faster. This suggests that eIFiso4E is more able to rapidly change conformation because of its smaller size. The much larger protein complex may have assumed an intermediate conformation that is able to form the stable complex quickly.

Our previous studies (*37*) have shown that eIF4B has a significant effect on the equilibrium for cap binding with eIFiso4F. The dissociation equilibrium constant decreased from 36.9 ± 0.49 to 29.0 ± 0.55 nM in the presence of eIF4B (*37*). Only a small effect on k_2 was observed for eIFiso4F·eIF4B (39.6 ± 1.1 s^{-1}) compared to eIFiso4F (37.9 s^{-1}) binding to a mononucleotide cap analogue. It is unlikely there is much effect on the initial second-order binding, because that rate is close to the diffusion-controlled rate and cannot account for the difference in the equilibrium constant. The difference resides in the dissociation rate, as was shown to be the case for eIFiso4F·PABP. Figures 6 and 7 show the time course for the dissociation reaction for four complexes. A significant difference in dissociation rate is seen in the presence of eIF4B and/or PABP for both the mononucleotide and dinucleotide cap analogue. The dissociation rates are at least 3.7- and 5.4-fold slower for eIFiso4F·Ant-m^{7}GTP and eIFiso4F·m^{7}GpppG in the presence of eIF4B and PABP, respectively.

Arrhenius activation energies for binding of eIFiso4F·4B and eIFiso4F·4B·PABP to Ant-m^{7}GTP were 53.27 ± 2.7 and 29.22 ± 1.32 kJ/mol, respectively. Addition of eIF4B to eIFiso4F and eIFiso4F·PABP lowered the activation energy as compared to our previous data of eIFiso4F alone and for the eIFiso4F·PABP complex (*38*). This reduced temperature dependence suggests that eIF4B or PABP succeeds in accelerating the reaction by providing a path with a substantially lower energy barrier.

The kinetic effects of eIF4B enhancement on cap affinity reside primarily in the dissociation rates. A likely possibility is that eIF4B and PABP, which interact with eIFiso4F, induce a conformational change that is propagated to the cap binding site. The lower activation energy of eIF4B suggests an intermediate that more easily achieves a stable conformation.

It is interesting to note how the temperature dependence of the kinetics leads to these different activation energies. PABP reduces the E_a for eIFiso4F by increasing the "on" rate, k_2, at low temperatures and decreasing it at high temperatures, effectively narrowing the range of rates over this temperature span. eIF4B has much the same effect as PABP on E_a, but is not quite as effective in lowering E_a as PABP. eIFiso4F·eIF4B has an ~13.5 kJ/mol higher E_a than eIFiso4F·PABP. The rates are affected by eIF4B in a manner similar to the effects of PABP. However, the combination of eIF4B and PABP shows further lowering of the activation energy. This ternary complex binds the cap with a lower activation energy than eIFiso4F·PABP or eIFiso4F·eIF4B; however, all rates (low to high temperatures) are enhanced compared to that with eIFiso4F·PABP. These data suggest that the combination of eIF4B and PABP produces a complex that not only has a low activation energy but also maintains a rapid binding of the cap to the complex. This complex will be able to form a stable intermediate with rapid cap binding and should substantially enhance the rate of protein synthesis. eIF4B and PABP interactions can exquisitely regulate responses of plants to temperature through cap binding. These data provide further insights into the formation of the translation initiation complex and form a basis for determining the detailed effects of protein phosphorylation and other plant responses to stress conditions.

REFERENCES

1. Sha, M., Wang, Y., Xiang, T., van Heerden, A., Browning, K. S., and Goss, D. J. (1995) Interaction of wheat germ protein synthesis initiation factor eIFiso4F and its subunits p28 and p86 with m^{7}GTP and mRNA analogues, *J. Biol. Chem. 270*, 29904−29909.
2. Jagus, R., Anderson, W. F., and Safer, B. (1981) The regulation of initiation of mammalian protein synthesis, *Prog. Nucleic Acids Res. Mol. Biol. 25*, 127−185.
3. Hershey, J. W. B. (1991) Translational control in mammalian cells, *Annu. Rev. Biochem. 60*, 717−755.
4. Mathews, M. B., Sonenberg, N., and Hershey, J. W. B. (1996) in *Translational Control* (Hershey, J. W. B., Mathews, M. B., and Sonenberg, N., Eds.) pp 1−29, Cold Spring Harbor Laboratory Press, Plainview, NY.
5. Standart, N., and Jackson, R. J. (1994) Regulation of translation by specific protein/mRNA interactions, *Biochimie 76*, 867−879.
6. Bi, X., and Goss, D. J. (2000) Wheat germ poly(A)-binding protein increases the ATPase and the RNA helicase activity of translation initiation factors eIF4A, eIF4B, and eIF-iso4F, *J. Biol. Chem. 275*, 17740−17746.
7. Jackson, R. J., and Standard, N. (1990) Do the poly(A) tail and 3′ untranslated region control mRNA translation, *Cell 62*, 15−24.
8. Munroe, D., and Jacobson, A. (1990) mRNA poly(A) tail, a 3′ enhancer of translational initiation, *Mol. Cell. Biol. 10*, 3441−3455.
9. Munroe, D., and Jacobson, A. (1990) Tales of poly(A): A review, *Gene 91*, 151−158.
10. Bernstein, P., and Ross, J. (1989) Poly(A), poly(A) binding protein and the regulation of mRNA stability, *Trends Biochem. Sci. 14*, 373−377.
11. Sonenberg, N. (1988) Cap-binding proteins of eukaryotic messenger RNA: Functions in initiation and control of translation, *Prog. Nucleic Acid Res. Mol. Biol. 35*, 173−207.
12. Rhoads, R. E. (1988) Cap recognition and the entry of mRNA into the protein synthesis initiation cycle, *Trends Biochem. Sci. 13*, 52−56.
13. Gallie, D. R., and Tanguay, R. L. (1994) Poly(A) binds to initiation factors and increases cap-dependent translation in vitro, *J. Biol. Chem. 269*, 17166−17173.
14. Tarun, S. Z., Jr., and Sachs, A. B. (1996) Association of the yeast poly(A) tail binding protein with translation initiation factor eIF4G, *EMBO J. 15*, 7168−7177.
15. Le, H., Tanguay, R. L., Balasta, M. L., Wei, C. C., Browning, K. S., Goss, D. J., and Gallie, D. R. (1997) Translation initiation factors eIFiso4G and eIF4B interact with the poly(A)-binding protein and increase its RNA binding activity, *J. Biol. Chem. 272*, 16247−16255.
16. Merrick, W. C. (1992) Mechanism and regulation of eukaryotic protein synthesis, *Microbiol. Rev. 56*, 291−315.
17. Gingras, A. C., Raught, B., and Sonenberg, N. (1999) eIF4 initiation factors: Effectors of mRNA recruitment to ribosomes and regulators of translation, *Annu. Rev. Biochem. 68*, 913−963.
18. Hershey, J. W. B., and Merrick, W. C. (2000) The pathway and mechanism of initiation of protein synthesis, in *Translational control of gene expression* (Sonenberg, N., Hershey, J. W. B., and Mathews, M. B., Eds.) pp 33−88, Cold Spring Harbor Laboratory Press, Plainview, NY.

19. Morley, S. J. (2001) The regulation of eIF4F during cell growth and cell death, in *Signaling pathways for translation* (Rhoads, R. E., Ed.) pp 1−37, Springer-Verlag, Berlin.
20. Gallie, D. R. (1998) A tale of two termini: A functional interaction between the termini of an mRNA is a prerequisite for efficient translation initiation, *Gene 17*, 1−11.
21. Wells, S. E., Hillner, P. E., Vale, R. D., and Sachs, A. B. (1998) Circularization of mRNA by eukaryotic translation initiation factors, *Mol. Cell 2*, 135−140.
22. Browning, K. S., Lax, S. R., and Ravel, J. M. (1987) Identification of two messenger RNA cap binding proteins in wheat germ. Evidence that the 28 kDa subunit of eIF4B and the 26 kDa subunit of eIF4F are antigenically distinct polypeptides, *J. Biol. Chem. 262*, 11228−11232.
23. Browning, K. S., Webster, C., Roberts, J. K., and Ravel, J. M. (1992) Identification of an isozyme form of protein synthesis initiation factor 4F in plants, *J. Biol. Chem. 267*, 10096−10100.
24. Balasta, M. L., Carberry, S. E., Friedland, D. E., Perez, R. A., and Goss, D. J. (1993) Characterization of the ATP-dependent binding of wheat germ protein synthesis initiation factors eIFiso4F and eIF4A to mRNA, *J. Biol. Chem. 268*, 18599−18603.
25. Wei, C. C., Balasta, M. L., Ren, J., and Goss, D. J. (1998) Wheat germ poly(A) binding protein enhances the binding affinity of eukaryotic initiation factor 4F and iso4F for cap analogues, *Biochemistry 37*, 1910−1916.
26. Lax, S. R., Fritz, W., Browning, K. S., and Ravel, J. M. (1985) Isolation and characterization of factors from wheat germ that exhibit eukaryotic initiation factor 4B activity and overcome 7-methylguanosine 5′-triphosphate inhibition of polypeptide synthesis, *Proc. Natl. Acad. Sci. U.S.A. 82*, 330−333.
27. Lax, S. R., Fritz, W., Browning, K. S., Maia, D. M., and Ravel, J. M. (1986) ATPase activities of wheat germ initiation factors 4A, 4B and 4F, *J. Biol. Chem. 261*, 15632−15636.
28. Lax, S. R., Lauer, S. J., Browning, K. S., and Ravel, J. M. (1986) Purification and properties of protein synthesis initiation and elongation factors from wheat germ, *Methods Enzymol. 118*, 109−128.
29. Abramson, R. D., Browning, K. S., Dever, T. E., Lawson, T. G., Thach, R. E., Ravel, J. M., and Merrick, W. C. (1988) Initiation factors that bind mRNA. A comparison of mammalian factors with wheat germ factors, *J. Biol. Chem. 263*, 5462−5467.
30. Tarun, S. Z., and Sachs, A. B. (1995) A common function for mRNA 5′ and 3′ ends in translation initiation in yeast, *Genes Dev. 9*, 2997−3007.
31. Ren, J., and Goss, D. J. (1996) Synthesis of a fluorescent 7-methylguanosine analog and a fluorescence spectroscopic study of its reaction with wheat germ cap binding proteins, *Nucleic Acids Res. 18*, 3629−3634.
32. van Heerden, A., and Browning, K. S. (1994) Expression in *Escherichia coli* of the two subunits of the isozyme form of wheat germ protein synthesis initiation factor 4F. Purification of the subunits and formation of an enzymatically active complex, *J. Biol. Chem. 269*, 17454−17457.
33. Bradford, M. M. (1976) A rapid and sensitive method for the quantitation of microgram quantities of protein utilizing the principle of protein-dye binding, *Anal. Biochem. 72*, 248−254.
34. Darzynkiewicz, E., Stepinski, J., Ekiel, I., Jin, Y., Haber, D., Sijuwade, T., and Tahara, S. M. (1988) β-Globin mRNAs capped with m^7G, m2.7(2)G or m2.2.7(3)G differ in intrinsic translation efficiency, *Nucleic Acids Res. 16*, 8953−8962.
35. Darzynkiewicz, E., Stepinski, J., Ekiel, I., Goyer, C., Sonenberg, N., Termeriusz, A., Jin, Y., Sijuwade, T., Haber, D., and Tahara, S. M. (1989) Inhibition of eukaryotic translation by nucleoside 5′-monophosphate analogues of mRNA 5′-cap: Changes in N7 substituent affect analogue activity, *Biochemistry 28*, 4771−4778.
36. Olsen, K., Christensen, U., Sierks, M. R., and Svensson, B. (1993) Reaction mechanisms of Trp120 → Phe and wild-type glucoamylases from *Aspergillus niger*. Interactions with maltooligodextrins and acarbose, *Biochemistry 32*, 9686−9693.
37. Khan, M. A., and Goss, D. J. (2004) Phosphorylation states of translational initiation factors affect mRNA cap binding in wheat, *Biochemistry 43*, 9092−9097.
38. Luo, Y., and Goss, D. J. (2001) Homeostasis in mRNA initiation: Wheat germ poly(A)-binding protein lowers the activation energy barrier to initiation complex formation, *J. Biol. Chem. 276*, 43083−43086.
39. Garland, D. L. (1978) Kinetics and mechanism of colchicines binding to tubulin: Evidence for ligand-induced conformational change, *Biochemistry 17*, 4266−4272.

BI047298G